Intracellular pH Controls Cell Membrane Na^+ and K^+ Conductances and Transport in Frog Skin Epithelium

BRIAN J. HARVEY, S. RANDALL THOMAS, and JORDI EHRENFELD

From the Département de Biologie du Commissariat à l'Energie Atomique, Laboratoire Jean Maetz, F-06230 Villefranche-sur-Mer, France

ABSTRACT We determined the effects of intracellular respiratory and metabolic acid or alkali loads, at constant or variable external pH, on the apical membrane Na^+-specific conductance (g_a) and basolateral membrane conductance (g_b), principally due to K^+, in the short-circuited isolated frog skin epithelium. Conductances were determined from the current-voltage relations of the amiloride-inhibitable cellular current pathway, and intracellular pH (pH_i) was measured using double barreled H^+-sensitive microelectrodes. The experimental set up permitted simultaneous recording of conductances and pH_i from the same epithelial cell. We found that due to the asymmetric permeability properties of apical and basolateral cell membranes to HCO_3^- and NH_4^+, the direction of the variations in pH_i was dependent on the side of addition of the acid or alkali load. Specifically, changing from control Ringer, gassed in air without HCO_3^- ($pH_o = 7.4$), to one containing 25 mmol/liter HCO_3^- that was gassed in 5% CO_2 ($pH_o = 7.4$) on the apical side caused a rapid intracellular acidification whereas when this maneuver was performed from the basolateral side of the epithelium a slight intracellular alkalinization was produced. The addition of 15 mmol/liter NH_4Cl to control Ringer on the apical side caused an immediate intracellular alkalinization that lasted up to 30 min; subsequent removal of NH_4Cl resulted in a reversible fall in pH_i, whereas basolateral addition of NH_4Cl produced a prolonged intracellular acidosis. Using these maneouvres to change pH_i we found that the transepithelial Na^+ transport rate (I_{sc}), and g_a, and g_b were increased by an intracellular alkalinization and decreased by an acid shift in pH_i. These variations in I_{sc}, g_a, and g_b with changing pH_i occurred simultaneously, instantaneously, and in parallel even upon small perturbations of pH_i (range, 7.1–7.4). Taken together these results indicate that pH_i may act as an intrinsic regulator of epithelial ion transport.

INTRODUCTION

In epithelia it has long been realized that variations in ion movements at opposing apical and basolateral cell membranes may influence each other. Such intrinsic regulation has been termed transcellular "cross-talk" or coupling and is known to

Address reprint requests to Dr. Brian J. Harvey, Laboratoire Jean Maetz, B.P. 68, Station Marine 06230 Villefranche-sur-Mer, France.

J. GEN. PHYSIOL. © The Rockefeller University Press · 0022-1295/88/12/0767/25 $2.00
Volume 92 December 1988 767–791

occur in a wide variety of epithelia (reviewed by Schultz 1981; and Diamond 1982). Definite evidence for cross-talk was first obtained from work on frog skin (MacRobbie and Ussing, 1961; Helman et al., 1979), toad urinary bladder (Finn, 1974; Reuss and Finn, 1975; Davis and Finn, 1982), and *Necturus* urinary bladder (Thomas et al., 1983). In the frog skin it was found that inhibition of the basolateral Na^+/K^+ ATPase was accompanied by a decrease in apical Na permeability and conductance. A converse type of cross-talk was described in the toad bladder where block of the apical Na^+ conductance was accompanied by a decrease in basolateral K^+ conductance, whereas in *Necturus* urinary bladder the basolateral membrane conductance was found to increase with the conductance of the apical membrane when Na^+ transport was stimulated. Another type of "parallel coupling" has been described within the basolateral membrane between "pump" (Na^+/K^+-ATPase) and "leak" (K^+ electrodiffusion). In renal proximal tubules ouabain inhibition of the Na^+/K^+ ATPase pump was accompanied by a parallel decrease in apparent K^+ conductance (Messner et al., 1985).

Up until now, however, the intracellular signal that controls cell membrane conductances has not been identified. In this study we examined the possibility that intracellular pH may act as such a signal.

Intracellular pH is closely regulated in animal cells and much information exists on the mechanisms that control pH_i within narrow limits (Roos and Boron, 1981; Thomas, 1984). In spite of the importance of this tight regulation of pH_i, considering its profound effects on cell properties, such as excitability and ion transport (for review see Moody, 1984), there is little information on the role of normal physiological or experimentally induced changes in pH_i in controlling cell membrane conductances, especially in epithelia. Experimental maneuvers designed to create an intracellular acid load have been shown to decrease the short-circuit current in frog skin (Funder et al., 1967; Mandel, 1978) and to decrease apical Na^+ permeability in the K^+-depolarized toad urinary bladder (Palmer, 1985). Furthermore, an intracellular acidification was reported to reduce the K^+ transference in the *Necturus* proximal tubule (Kubota et al., 1983) and in cultured bovine retinal pigment cells (Keller et al., 1986). Since no quantitative study has yet been reported on these responses, our aim was to characterize the effects of respiratory and metabolic acid-base disturbances on pH_i in the short-circuited isolated frog skin epithelium and, having done so, to study the effects of such experimentally induced changes in pH_i on apical Na^+ and basolateral K^+ conductances.

In the companion paper (Harvey and Ehrenfeld, 1988) we report on the evidence for Na^+/H^+ exchange at the basolateral membrane and its role in pH_i regulation, and, as a consequence, the effect of its activity on Na^+ and K^+ conductances.

GLOSSARY

Current is expressed in units of $\mu A \cdot cm^{-2}$ surface area, voltage in mV, and conductance in $mS \cdot cm^{-2}$.

I_{sc}: short-circuit current.

I_t: transepithelial clamp current.

I_a, I_b: amiloride-sensitive current across the apical and basolateral cell membranes, respectively.

V_t: transepithelial potential difference.
V_a: apical cell membrane potential.
V_b: basolateral cell membrane potential.
V_R: reversal potential, equivalent to Nernst potential for passive Na^+ distribution across the apical membrane. Determined from $I_a - V_a$ relations at V_a when $I_a = 0$.
g_a: slope conductance of the amiloride-sensitive Na^+ transport pathway at the apical membrane. Determined from the partial derivative of the Goldman-Hodgkin-Katz (GHK) flux equation.
P_{Na}: apical membrane Na^+ permeability determined from GHK fit to $I_a - V_a$ relations.
g_b: slope conductance of the basolateral membrane determined from linear regression analysis of $I_b - V_b$ relations.
G_{Na}: chord conductance of the amiloride-sensitive Na transport pathway at the apical membrane.
G_t: total transepithelial conductance.
G_c: transcellular conductance; (G_t in absence of amiloride) − (G_t in presence of 50 μM amiloride in apical bath).
G_a, G_b: apical and basolateral membrane conductance, respectively, obtained from circuit analysis.
R_a, R_b: reciprocal of G_a and G_b (resistance)
$F(R_a)$: fractional resistance of apical membrane, equivalent to G_c/G_a.
$[Na^+]_i$: intracellular sodium concentration calculated from V_R at constant external apical sodium concentration.
pH_i: intracellular pH measured with double-barreled ion-sensitive microelectrodes.
$[K^+]_b$: potassium concentration in the basolateral Ringer solution.

METHODS

The experiments were carried out on in vitro *Rana esculenta* ventral skin ("whole skin") and on the epithelium ("isolated epithelium") isolated by treating the corial side with 1.0 mg/ml collagenase (Worthington Biochemical Corp., St. Louis, MO) at 30°C under a 10-cm hydrostatic pressure. The whole skin or isolated epithelium was mounted in a modified Ussing chamber that permitted cell penetration from above, via either the apical or basolateral sides, by microelectrodes. The transepithelial potential (V_t) was clamped to zero by short-circuiting the tissue using an automatic voltage clamp (model VC600; Physiologic Instruments, Houston, TX). The Na^+ transport rate was measured as being equivalent to the short-circuit current (I_{sc}), which was sensitive to amiloride (50 μM) applied to the apical side.

Solutions and Drugs

The tissue was normally perfused on both sides with a Ringer solution designated "control" in the text, which had the following composition (in millimolar): 83 NaCl, 2.5 KCl, 2 $CaCl_2$, 11 Na_2SO_4, 2 $MgSO_4$, 1.2 KH_2PO_4, 2.5 Na_2HPO_4, 11 glucose. This solution was gassed in air and buffered to pH 7.4 with BES (10 mM), pH adjustment was made with 1 N NaOH (when 1 mM $BaCl_2$ was added to the basolateral side, this Ringer solution had sulfate salts replaced by the corresponding chloride salt). When intracellular acid-base disturbances were produced at constant external pH, the control Ringer on the apical side was changed for a Ringer of similiar composition except that it was gassed in 5% CO_2 and contained 24 mM $NaHCO_3$ in place of the 11 mM Na_2SO_4. Alternatively, an intracellular alkalinization or acidification was produced at constant external pH by adding 15 mM NH_4Cl to the control Ringer on the apical or basolateral side.

Amiloride was purchased from Merck, Sharp and Dohme (West Point, PA) and 4.4'-diisothiocyanostilbene-2-2'disulfonic acid (DIDS) from Sigma Chemical Co. (St. Louis, MO).

Microelectrode Recording Arrangements

Apical and basolateral cell membrane potential differences (V_a and V_b, respectively) were recorded with borosilicate glass (Hilgenberg, FRG) microelectrodes filled with 1 M KCl (60–80 MΩ tip resistance when immersed in Ringer solution) and connected via Ag/AgCl wire to a dual microprobe amplifier (model 750; World Precision Instruments (WPI), New Haven, CT). Current and potential differences were measured with reference to the apical Ringer solution connected to virtual ground in the VC 600 clamp. Microelectrodes were advanced into the cells using Huxley Goodfellow micromanipulators (HG-3000; Goodfellow Metals, Cambridge, UK).

pH_i was measured with double-barreled H^+ ion-sensitive microelectrodes using the proton ionophore tridodecylamine as the H^+ sensor (Proton cocktail 82500; Fluka, Switzerland). Manufacture and calibration of pH microelectrodes was similar to that described previously (Harvey and Ehrenfeld, 1986) and is described in greater detail in the companion paper. The electrodes responded with non–Nernstian slopes of 50–54 mV per pH unit when tested in calibration solutions over the pH range 5–8. The reference barrel was filled with 1 M KCl and was used to measure V_a or V_b.

The ion-sensitive barrel was backfilled with 1 M NaCl and Na citrate at a pH of 6.5. This latter barrel, when present within a cell and referenced to the external Ringer solution, measures the transmembrane electrochemical potential for H^+ when corrected for the non–Nernstian calibration response. The outputs from the reference and ion-sensitive barrels were fed via Ag/AgCl wires to a high input impedance differential electrometer (FD 223; NPI) and then sent to a driven shield (FC 23; WPI) around the microelectrode. We used double-barreled ion-sensitive microelectrodes in preference to two separate single barrels. The accurate recording of pH_i requires subtraction of the membrane potential output of both reference and ion-sensitive barrels, and this is best obtained when both barrels record from the same cell.

Membrane potentials were displayed on an oscilloscope (model 5115; Tektronix, Inc., Beaverton, OR), and I_{sc}, cell membrane potentials and pH_i were monitored on a potentiometric pen recorder (type 2065; Linseis, FRG), and stored on floppy disk by an Apple IIe computer, or on hard disk by an IBM AT 3 computer using a Unisoft program.

Current-Voltage Analysis

The recording of current-voltage (*I-V*) curves was performed under short-circuit current conditions with a computer program adapted from the one used by Thomas et al. (1983) and an Apple IIe computer for data storage and analysis. The current-pulse train consisted of transepithelial bipolar current pulses (I_t) of 50-ms duration, 100-ms interval between pulses, and of sufficient strength to clamp the V_t over the range 0 to ±200 mV in steps of 5, 10, or 20 mV under computer command.

The *I-V* relations of the apical membrane amiloride-sensitive Na^+ conductive pathway (I_a-V_a) were obtained from the difference in the I_t-V_a curves recorded under control spontaneous Na^+ transport conditions and those recorded when I_{sc} had fallen to a steady level between 30–90 s after the addition of 50 μM amiloride to the apical Ringer solution. We assume that the amiloride-inhibited I_{sc} is equal to the transcellular Na^+ current pathway. For short applications of amiloride this assumption appears valid for a wide variety of tight-junctioned epithelia (Thompson et al., 1982; Nagel et al., 1983; Thomas et al., 1983). In agreement with recent reports in whole frog skin (De Long and Civan, 1984; Schoen and Erlij, 1985), the I_a-V_a relationship recorded in whole skin or isolated epithelium could be accurately described

by the GHK equation for a single permeant ion (Na^+) over the range of V_a between -200 and $+100$ mV.

The GHK flux equation (Eq. 1) was fitted to the I_a-V_a relations by obtaining the best-fit values for apical Na^+ permeability (P_{Na}) and cell sodium concentration ($[Na]_i$)

$$I_a = -\left(\frac{P_{Na} \cdot V_a \cdot F^2}{RT}\right)\left(\frac{[Na]_o - [Na]_i \exp(x)}{1 - \exp(x)}\right), \quad (1)$$

where $x = V_a \cdot F/RT$. The slope conductance of the amiloride-sensitive apical Na^+ transport pathway (g_a) was calculated from the following differential forms of the GHK equation: for g_a at any V_a, except $V_a = 0$

$$\frac{dI}{dV} = \left\{\frac{F^2 \cdot P_{Na}}{RT}\right\}\left\{\frac{[\exp(x)(1 - x) - 1][[Na]_i \exp(x) - [Na]_o]}{[\exp(x) - 1]^2} + [x/(\exp\{x\} - 1)] \cdot [[Na]_i \exp(x)]\right\}. \quad (2)$$

For g_a at $V_a = 0$:

$$\frac{dI}{dV} = \left(\frac{F^2 \cdot P_{Na}}{RT}\right)\left(\frac{[Na]_o + [Na]_i}{2}\right). \quad (3)$$

For g_a at the reversal potential:

$$\frac{dI}{dV} = \left(\frac{F^2 \cdot P_{Na}}{RT}\right)\left(\frac{[Na]_o \cdot [Na]_i}{[Na]_o - [Na]_i} \cdot \ln\frac{[Na]_o}{[Na]_i}\right). \quad (4)$$

An alternative measure, used by some workers, of apical membrane Na^+ conductance is the chord conductance (G_{Na}), which relates the measured transcellular Na^+ current to the transmembrane Na^+ electrochemical driving force ($\Delta\tilde{\mu}Na$). G_{Na} was determined from Eq. 5.

$$G_{Na} = I_a/\Delta\tilde{\mu}Na = I_a/(V_a - V_R) = \left\{\frac{F^2 \cdot P_{Na} \cdot x}{RT}\right\}\left\{\frac{[Na]_o - [Na]_i \exp(x)}{[1 - \exp(x)] - [\ln [Na]_o/[Na]_i]}\right\}. \quad (5)$$

In general, we chose to determine the slope conductance at $V_a = V_R$ since the chord and slope conductances are closely related only in the range of membrane voltages near the reversal potential (Thompson, 1986).

The *I-V* relations of the basolateral cell membranes (I_b-V_b) were recorded simultaneously with those of the apical membrane I_a-V_a relations and were obtained from the difference between those determined before and after the addition of amiloride (50 μM) to the apical bath. These "difference" I_b-V_b relations were linear and stabilized for sample times >20 ms after the onset of the voltage clamp, which is in agreement with the observations of Schoen and Erlij (1985). The slope conductance of the basolateral membranes (g_b) was calculated from linear regression analysis of the difference I_b-V_b relations over the range of basolateral membrane voltage of 0 and 150 mV.

Apparent Relative K^+ Conductance

To a large extent, g_b reflects K^+ conductance since this membrane is K^+ permselective. We attempted to estimate the relative K^+ conductance of the basolateral cell membranes by determining the K^+-dependent partial potential ratio T_K:

$$T_K = \Delta V_b \frac{RT}{F} \ln\frac{[K]_t}{[K]_c}, \quad (6)$$

where ΔV_b is the response of the basolateral membrane potential (under short-circuit conditions) to the sudden increase in the K^+ concentration of the basolateral Ringer from $[K]_c$ = 3.7 to $[K]_t$ = 37 mM made by adding K gluconate or KCl.

The apparent relative rubidium conductance was calculated in the same manner as the T_K by substituting all K^+ with Rb^+ in the control Ringer and then adding 33.3 mM RbCl to the test solution.

It is more correct to consider K^+ transference (t_K) rather than K^+-dependent partial potential ratio (T_K) as indicative of the apparent relative K^+ conductance, since t_K is calculated from changes in basolateral membrane electromotive force rather than membrane potential. From equivalent circuit analysis in open-circuit conditions t_K = 0.97 ± 0.03 (n = 8), and in short-circuit conditions t_K = 0.94 ± 0.04 (n = 8). Thus, the basolateral membrane is K^+ permselective. The normalized values of T_K/T_K max and t_K/t_K max showed the same relative change as a function of pH; for this reason we used the more easily determined T_K as an expression of variations occurring in K^+ conductance.

Circuit Analysis

In some experiments when we were not measuring *I-V* relations we obtained a measurement of apical and basolateral membrane conductances (G_a and G_b, respectively) by an equivalent circuit analysis (Schultz et al., 1977). This method requires measurements of the fractional resistance of the apical membrane (FR_a) and of the transcellular conductance (G_c).

The FR_a was determined from the voltage divider $\Delta V_a/\Delta V_t$ measured from the displacement of V_a when V_t was voltage clamped to ±10 mV under short-circuit current conditions. The difference between the transepithelial conductance (G_t) measured before and after block of I_{sc} with amiloride was assumed to give the transcellular conductance (see Nagel et al., 1983 for criticism). These measurements of FR_a were performed for 500 ms every 5 s in the absence or presence of apical amiloride (50 μM), and were displayed and stored by the computer. From this analysis we obtain:

$$FR_a = \Delta V_a/V_t = G_c/G_a \tag{7a}$$

$$G_a = G_c/FR_a \tag{7b}$$

$$G_b = G_c/(1 - FR_a) \tag{7c}$$

Cell impalements were accepted if FR_a approached unity after the addition of amiloride (50 μM) to the apical Ringer solution.

^{22}Na Unidirectional Flux

The transepithelial unidirectional sodium fluxes were measured in whole frog skin with the isotope ^{22}Na (0.2 μCi/ml) added to the mucosal solution. After a 20-min equilibration period, the appearance of the isotope was followed in the serosal solution as a function of time with an automatic gamma-counter (MR 252; Kontron, France). The fluxes were calculated in nanoequivalents per $hour^{-1}$ per $centimeters^2$ and compared with simultaneous measurements of short-circuit current. Data are expressed as mean values ± SE of the mean and n is the number of experiments.

RESULTS

Intracellular Acid-Base Disturbances

In these experiments, we used, where indicated, the short-circuited whole frog skin or isolated epithelium when acid-base disturbances were produced from the apical

side, and we always used the isolated epithelium when these perturbations were made from the basolateral side. Control conditions mean that the tissue was superfused on both sides with bicarbonate-free Ringer equilibrated with air and buffered to pH 7.4 with BES (*N,N*-bis[2-hydroxyethyl]-2 aminoethane sulfonic acid).

CO_2:HCO_3^- Load

When the control Ringer bathing the apical side of the isolated epithelium was switched to one buffered in 5% CO_2 and 24 mmol/liter HCO_3^-, at constant external

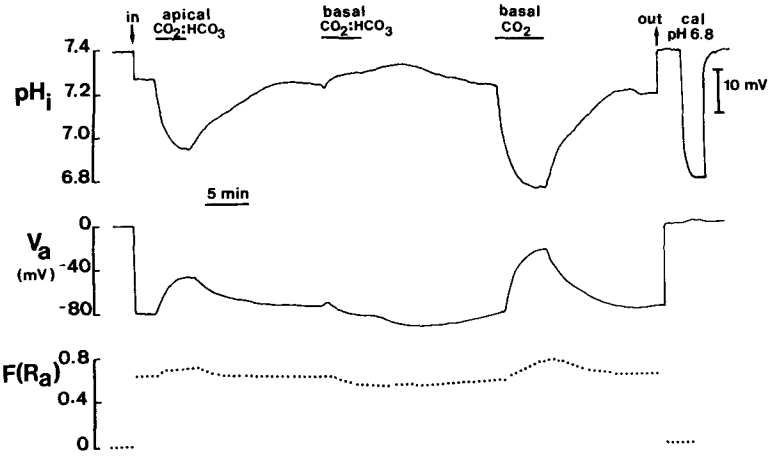

FIGURE 1. Recording of pH_i and apical membrane potential measured using a double-barreled H^+-sensitive microelectrode in an isolated epithelium under short-circuit current conditions. The fractional resistance (FR_a) was determined from equivalent circuit analysis and is the ratio of apical to transcellular resistances. The electrode entered a cell from the apical side at arrow "in" and recorded a pH_i of 7.27 and membrane potential of −80 mV. When control Ringer (equilibrated in air and buffered with BES to pH 7.4) on the apical side was switched to a Ringer buffered to the same pH with 5% CO_2 and 24 mM HCO_3^-, the pH_i fell rapidly to 6.85 and V_a depolarized with a small increase in FR_a. The pH_i recovered to normal values over a period of 10 min after return to the control Ringer. On the contrary, superfusion of CO_2:HCO_3^- Ringer on the basolateral side had little effect on pH_i producing only a slight alkalinization, which increased further immediately after return to control Ringer. The opposite effects of apical and basolateral CO_2:HCO_3^--buffered Ringer on pH_i may be due to HCO_3^- ions being permeable only at the basolateral membranes. In support of this conclusion it can be seen that superfusion of the basolateral side with Ringer gassed in 5% CO_2 without HCO_3^- (pH_b 6.4) produced a reversible fall in pH_i, comparable to that produced by apical CO_2:HCO_3^--buffered Ringer. After removal of the electrode from the cell (at arrow "out"), the electrode was calibrated by switching to a Ringer buffered to pH 6.8 with MES.

pH (7.4), an immediate and prolonged intracellular acidification was produced (Fig. 1). This marked fall in pH_i was readily reversible upon return to control Ringer. By contrast, when the basolateral side of the epithelium was superfused with the same CO_2:HCO_3^--buffered Ringer, the pH_i increased slightly (Fig. 1). The relative lack of effect of basolateral CO_2 on pH_i in this case is probably due to simultaneous CO_2

and HCO_3^- entry across the basolateral membrane and a subsequent increase in intracellular buffering power. In support of this conclusion we found that superfusion of the basolateral side with a Ringer equilibrated in 5% CO_2 without HCO_3^- (pH 6.4) caused a rapid and reversible cell acidification (Fig. 1). Since apical CO_2:HCO_3^--buffered Ringer produced similiar effects on pH_i, the HCO_3^- permeability of the apical cell membranes must be low.

Concomitant with the changes in pH_i, the intracellular potential also varied. Since the experiments were carried out under short-circuit current conditions this change

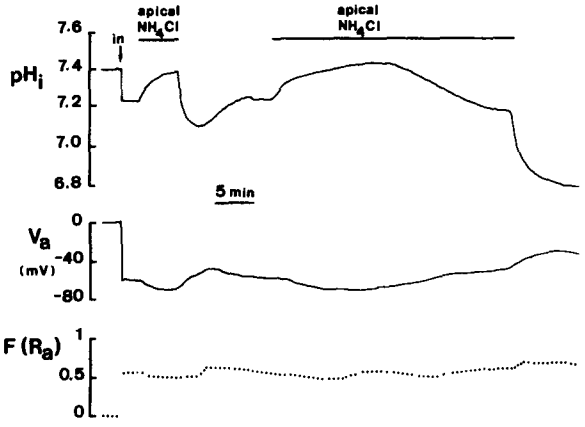

FIGURE 2. Recording of the effects of NH_4Cl (15 mM) on pH_i measured by a double-barreled H^+-sensitive microelectrode in the short-circuited frog skin. The electrode penetrated a cell from the apical side (at arrow "in") recording a pH_i of 7.21 and a membrane potential of −60 mV. The pH_i increased to 7.39 when 15 mM NH_4Cl was added from the apical side of constant external pH. Subsequent removal of NH_4Cl produced a "rebound" intracellular acidification. The effects of NH_4Cl on pH_i were time dependent and for long-term exposure the "plateau phase" alkalinization was followed, after a lapse of ~15 min, by a fall in pH_i. Subsequent removal of NH_4Cl produced an enhanced rebound acidification followed by a slow recovery phase. Despite the large changes in pH_i, there was little variation in the fractional resistance of the apical membrane.

in potential reflects variations in both apical and basolateral membrane potentials. Surprisingly, however, the ratio of apical to transcellular resistances (FR_a) changed only slightly. Thus, if changes in transcellular resistance occurred during perturbations of pH_i, the resistances of both the apical and basolateral membranes must have been affected simultaneously and in the same direction.

NH_3/NH_4^+ Load

To cause intracellular acid-base disturbances, we followed the now classical method described for other tissues of using an NH_4Cl prepulse to alkalinize the cell followed

by its washout to create a rebound intracellular acidification. Exposure of the apical side to 15 mM NH_4Cl in whole frog skin was associated with a rapid and transient intracellular alkalinization that lasted between 15 and 30 min (Fig. 2). For incubation periods longer than 15 min, we observed a decrease in pH_i. Upon removal of NH_4Cl the pH_i rapidly acidified and then recovered slowly to control values (Fig. 2). The degree of this acidification depended on the duration of exposure to NH_4Cl. An incubation time of at least 30 min was found to produce the maximum acidification after washout.

Exposure of the basolateral side to NH_4Cl (15 mM) in isolated epithelia produced a similar but faster pattern of pH_i changes to that observed during NH_4Cl addition on the apical side. During the first 2 min of exposure to NH_4Cl a rapid and tran-

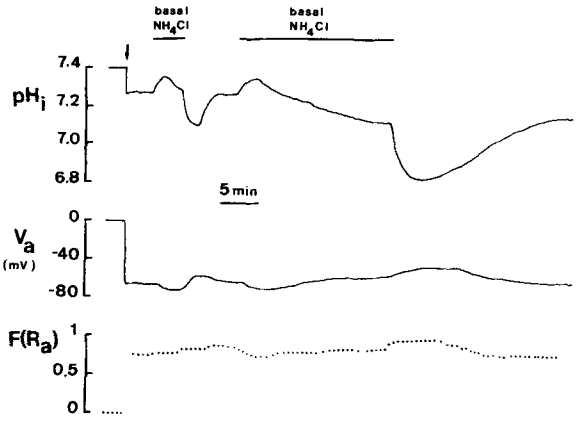

FIGURE 3. Double-barreled H^+-sensitive microelectrode recording of pH_i and membrane potential in the short-circuited isolated epithelium when NH_4Cl (15 mM) was added from the basolateral side. The cell impalement from the basolateral side is indicated by the arrow. The variations in pH_i appear similar to but faster than those seen in Fig. 2 for apical exposure to the weak base. The plateau-phase alkalinization, however, is reduced in both magnitude and in time course, and the subsequent fall in pH_i begins much earlier. Recovery from the rebound acidification after washout of basolateral NH_4Cl took longer than that produced from the apical side.

sient intracellular alkalinization was produced (Fig. 3). For longer incubation times, the pH_i slowly decreased to more acidic values. After washout of the NH_4Cl, the pH_i fell even further before returning to control levels. In both cases of NH_4Cl addition to the apical or basolateral Ringer, the disturbances in pH_i were accompanied by changes in membrane potential without a great deal of variation in FR_a (Figs. 2 and 3).

The degree of intracellular acidification produced by apical CO_2 or basolateral NH_4^+ was dependent on the intracellular buffering power (see Appendix). The latter was increased approximately twofold when a CO_2:HCO_3-buffered Ringers solution was present on the basolateral side. In this condition, gassing with CO_2 on the apical side or the addition of NH_4Cl to the basolateral side produced only very slight changes in pH_i. Thus, to produce sizeable variations in intracellular pH, the Ringer

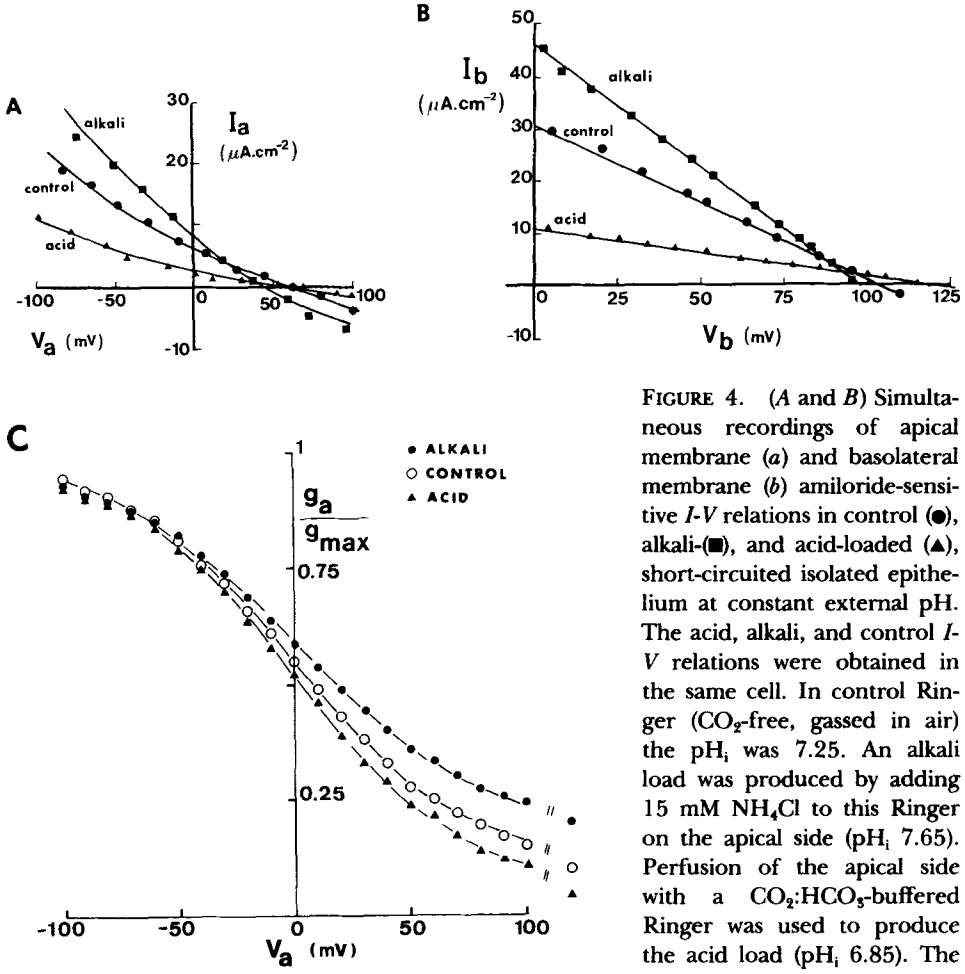

FIGURE 4. (*A* and *B*) Simultaneous recordings of apical membrane (*a*) and basolateral membrane (*b*) amiloride-sensitive *I-V* relations in control (●), alkali-(■), and acid-loaded (▲), short-circuited isolated epithelium at constant external pH. The acid, alkali, and control *I-V* relations were obtained in the same cell. In control Ringer (CO_2-free, gassed in air) the pH_i was 7.25. An alkali load was produced by adding 15 mM NH_4Cl to this Ringer on the apical side (pH_i 7.65). Perfusion of the apical side with a CO_2:HCO_3-buffered Ringer was used to produce the acid load (pH_i 6.85). The alkali load shifted both apical and basolateral membrane *I-V* curves, producing an increase in slope conductance and current at any given membrane potential. An acid load produced the opposite effects. Detailed characteristics of the GHK fit to the apical membrane *I-V* curves and linear regression analysis of the basolateral membrane *I-V* relations of such acid- and alkali-loaded cells are given in Table I. (*C*) Relations between g_a and V_a that were normalized by dividing g_a by its maximum theoretical value calculated from Eq. 8 under control conditions (○) and acid (▲) or alkali (●) loads. Since g_a/g_{max} vs. V_a relations under all three conditions are superimposable over the normal range of membrane voltages (−100 to −20 mV), the effect of pH_i on g_a is voltage independent. In other words, the degree of inhibition of g_a by low pH_i or stimulation by high pH_i is practically constant over the range of negative membrane potentials. This does not appear to be true for positive membrane potentials that are not normally encountered in the transporting epithelium. The maximum theoretical deviation from the voltage independence of the pH_i effect shown at large and positive V_a values was calculated from Eq. 9. At a large and negative V_a value:

$$\max dI/dV = (F^2 \cdot P_{Na}/RT) \cdot [Na]_i \tag{8}$$

At a large and positive V_a value:

$$\min dI/dV = (F^2 \cdot P_{Na} \cdot [Na]_o)/RT \tag{9}$$

bathing the basolateral side must contain a nonpermeable buffer. It should be noted that application of CO_2 from the apical side was found to be the most effective way of producing a rapid intracellular acidification that remained at a steady level during the presence of CO_2. On the other hand, the production of an alkaline shift in pH_i was best obtained during the first 20 min of exposure to NH_4Cl from the apical side. The response of pH_i to apically applied CO_2 or NH_4Cl was similiar in experiments on whole skin and on the isolated epithelium.

An intracellular acid load could also be effectively produced after the washout of NH_4Cl after preloading from the apical or basolateral sides. Moreover, a slowly changing acidification was best observed during long-term exposure (>5 min) of the isolated epithelium to NH_4Cl from the basolateral side.

These methods of creating intracellular acid-base disturbances at constant external pH allowed us to examine the effects of pH_i variations on the *I-V* relations and ionic conductances of the apical and basolateral cell membranes.

TABLE I

Effects of Intracellular Alkali and Acid Loads on Na^+ Transport Parameters

Condition	I_{sc}	P_{Na}	g_a	G_{Na}	g_b	$[Na]_i$	pH_i
	$\mu A \cdot cm^{-2}$	$10^{-6}\ cm \cdot s$	$mS \cdot cm^{-2}$	$mS \cdot cm^{-2}$	$mS \cdot cm^{-2}$	$mmol \cdot liter^{-1}$	
Control ($n = 8$)	20 ± 2	0.569 ± 0.067	0.156 ± 0.019	0.166 ± 0.017	0.29 ± 0.04	11 ± 2	7.23 ± 0.09
Alkali load ($n = 8$)	25 ± 2	0.853 ± 0.075	0.432 ± 0.036	0.307 ± 0.041	0.45 ± 0.04	23 ± 3	7.65 ± 0.11
Acid load ($n = 8$)	3 ± 0.5	0.265 ± 0.011	0.039 ± 0.005	0.036 ± 0.004	0.08 ± 0.01	5 ± 2	6.85 ± 0.25

Apical Na^+ permeability (P^{Na}), slope (g_a) and chord (G_{Na}) conductance, basolateral membrane slope conductance (g_b) and intracellular Na^+ concentration $[Na^+]_i$ were determined from amiloride-sensitive cell *I-V* relations. pH_i was measured using double-barreled H^+-sensitive microelectrodes. Control conditions were in bicarbonate-free Ringer solutions bathing both sides of the frog skin. An intracellular alkali load was induced by adding 15 mM NH_4CL to the control Ringer solution on the apical side. The *I-V* relations were recorded between 2 and 15 min after NH_4CL addition when pH_i and short-circuit current (I_{sc}) had reached stable maximum values. An intracellular acid load was produced by switching the control Ringer solution bathing the apical side to a solution buffered at the same pH with 5% CO_2 and 24 mM HCO_3^-. Data analysis was performed between 2 and 5 min after CO_2 equilibration when pH_i and I_{sc} had reached stable minimum values.

Effects of pH_i on Apical Membrane Na^+ Conductance and Basolateral Membrane Conductance at Constant External pH

The amiloride-sensitive *I-V* relationship of the apical cell membranes could be accurately fit by the GHK flux equation for Na^+ in control and in conditions of acid-base disturbances (Fig. 4 *A*). Using the equation as described in the Methods, we calculated apical Na permeability (P_{Na}), slope conductance (g_a), chord conductance (G_{Na}), and $[Na]_i$ when the cells were acid or alkali loaded (Table I). The effects of acid and alkali load on the *I-V* relationships of the apical Na conductive pathway and of the basolateral cell membranes recorded in the same cell of an isolated epithelium are shown in Fig. 4, *A* and *B*. An alkali load (produced by NH_4Cl addition to the apical side) always increased P_{Na}, g_a, Na transport rate (I_{sc}), and basolateral conductance (Table I) whereas a respiratory acid load (produced by CO_2:HCO_3 added to apical side) had the opposite effects on all of these parameters (Table I).

Voltage Independence of the pH_i Effect

The membrane potential changed with variations in pH_i, and, since the experiments were conducted under short-circuit conditions, the direction and magnitude of this change depended on both apical and basolateral membrane conductances. For example, inhibition of apical Na^+ entry would tend to hyperpolarize the apical membrane, whereas block of K^+ channels at the basolateral membrane would depolarize V_b. Do these voltage changes influence the effects of pH_i on apical membrane Na^+ conductance? With dissimilar concentrations of Na^+ on either side of the membrane, a voltage dependence of g_a is implicit in the GHK curves shown in Fig. 4 *A* and can be calculated from the first derivative of the *I-V* plot as a function of voltage (Eqs. 2–4). When plots of g_a vs. V_a were normalized by dividing g_a by the maximum (theoretical) value of g_a calculated for a large and negative V_a, the relations of g_a/g_{max} vs. V_a were found to be practically superimposable for control, alkali, and acid load conditions over the V_a range of -100 to -20 mV (Fig. 4 *C*). Thus, the voltage dependence of g_a was not distorted by intracellular acidification or alkalinization over the normal intracellular voltage range. Moreover, the relative inhibition or stimulation of g_a by acid or alkali loads, respectively, was constant over the V_a range normally encountered, indicating that the effects of intracellular H^+ on g_a were not affected by membrane potential changes.

Dependence of g_a on pH_i

Simultaneous measurements of pH_i and g_a using double-barreled H^+-sensitive microelectrodes and *I-V* analysis revealed a close covariance between these parameters. An intracellular acid load produced by CO_2: HCO_3^--buffered Ringer on the apical side was accompanied by a decrease in g_a and short-circuit current (Fig. 5). Upon return to control Ringer, the g_a and I_{sc} both increased in parallel with the recovery of pH_i to control values. The change in I_{sc} is expected to follow g_a if the apical Na^+ entry step is rate-limiting for overall transepithelial Na^+ transport. On the other hand, both g_a and I_{sc} were increased when CO_2:HCO_3^- Ringer was present either simultaneously on both sides or on the basolateral side alone. These changes were accompanied by a slight intracellular alkalinization (Fig. 5).

The effects of a long-term increase in pH_i on g_a and I_{sc} were investigated in the presence of NH_4Cl on the apical side. Immediately after the addition of 15 mmol/liter NH_4Cl, the g_a and I_{sc} increased in parallel with the rise in pH_i and remained at a steady level during the "plateau-phase" alkalinization (Fig. 6). After a 20-min incubation with NH_4Cl, the pH_i began to decline, as did the g_a and I_{sc}. After washout of NH_4Cl, the "rebound" acidification was accompanied by a decrease in g_a and I_{sc}, and subsequently these parameters showed a similar time-dependent recovery. The dependence of g_a and I_{sc} on pH_i variations in both alkaline and acidic directions could also be observed in the same cell by loading from the basolateral side with NH_3:NH_4^+. The addition of 15 mmol/liter NH_4Cl to the basolateral side produced a similar but much faster pattern of changes in pH_i, g_a, and I_{sc} (Fig. 7) than when NH_4Cl was present on the apical side. Again, the variations in g_a and I_{sc} were covariant with the induced perturbations in pH_i. The effect of NH_4Cl on pH_i and transport parameters was greatly diminished when the basolateral side was superfused in CO_2:HCO_3^--buffered Ringer (Fig. 7), a condition in which intracellular buffering

power is more than double that found in control BES-buffered Ringer (cf. Appendix). This result emphasizes the role of permeable buffers in dampening the effects of acid or alkali loads on pH_i and, as a consequence, on Na^+ transport.

The relationship obtained between g_a and pH_i determined in these experiments is given in Fig. 8. The specific Na^+ conductance of the apical cell membranes was

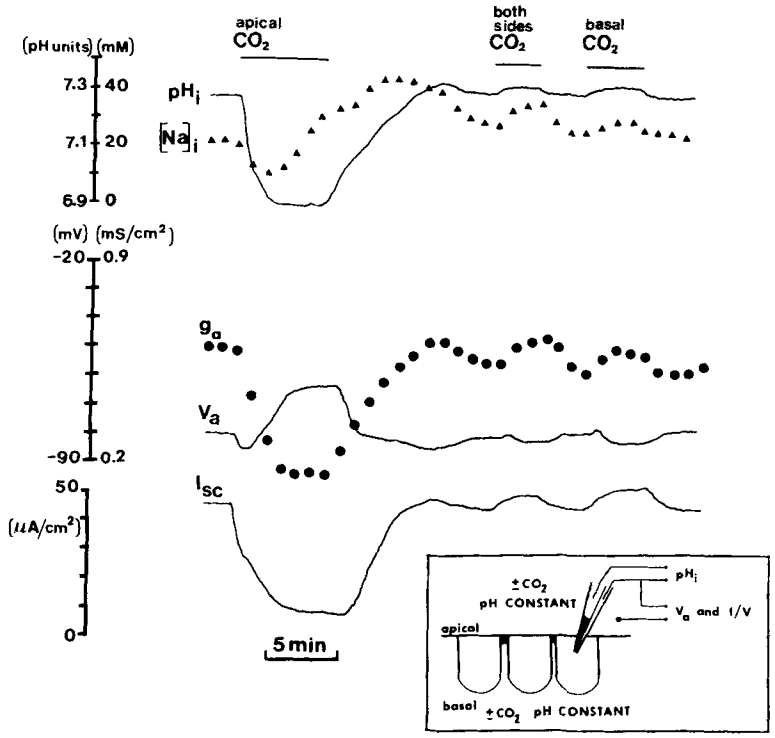

FIGURE 5. Response of pH_i, V_a, g_a, $[Na^+]_i$, and I_{sc} to substitution of control Ringer (HCO_3^- free equilibrated in air, pH 7.4) with Ringer gassed in 5% CO_2 containing 24 mM HCO_3^- (pH 7.4) on the apical or basolateral side of an isolated epithelium. The pH_i and V_a were measured with a double-barreled H^+-sensitive microelectrode, g_a and $[Na^+]_i$ were calculated from the GHK fit of amiloride-sensitive *I-V* relations at ~60-s intervals. For clarity the deflections in V_a and I_{sc} during the determination of the *I-V* relations that lasted 2 s have been blanked out. Application of a CO_2/HCO_3 Ringer to the apical side caused a rapid covariant and reversible decrease in pH_i, g_a, and I_{sc}. The V_a hyperpolarized and subsequently depolarized and calculated $[Na^+]_i$ fell initially and then increased during the intracellular acidification phase. Perfusion of CO_2:HCO_3 Ringer solution on both sides or solely on the basolateral side had the opposite effects, causing a slight intracellular alkalinization and an increase in g_a and I_{sc}. The inset shows the experimental protocol.

found to be a steep sigmoidal function of pH_i, especially over the physiological range of pH_i values between 7.1 and 7.4 where g_a varied 10-fold. The maximum value of g_a was obtained at a pH_i of 8.0 and the minimum at pH_i 6.5.

The relation g_a/g_{max} vs. pH_i could be described by a titration curve fit by the equation $g_a/g_{max} = K^n/(K^n + [H]_i^n)$, where $K = 10^{-pK}$ and n is a binding constant (Moody

and Hagiwara, 1982). The best fit was obtained with a pK of 7.25 and $n = 2$ (Fig. 8).

From I_a-V_a relations, we also calculated apical P_{Na}, G_{Na}, and $[Na]_i$ (from the reversal potential). An intracellular acid load always reduced P_{Na} and G_{Na} (Table I), whereas its effects on $[Na]_i$ were biphasic. $[Na]_i$ tended to decrease during the first 5

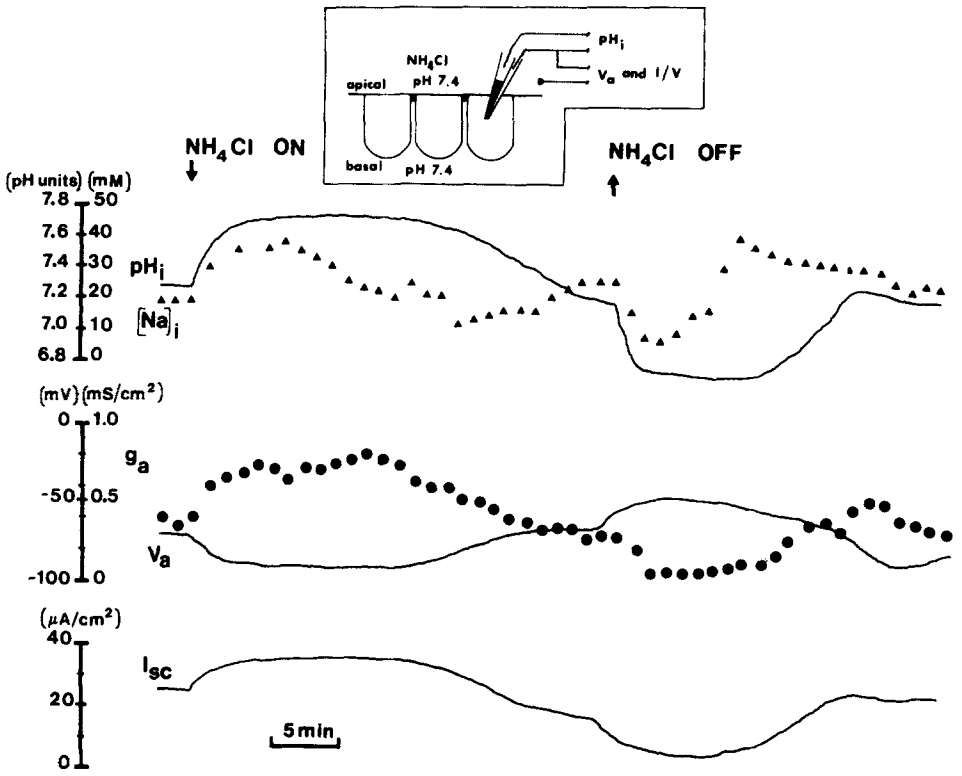

FIGURE 6. Effects of the addition of 15 mM NH_4Cl (to the apical side of frog skin), at a constant external pH of 7.4 on pH_i and $[Na^+]_i$ membrane potential, amiloride-sensitive apical Na^+ conductance and short-circuit current. Cell impalement was from the apical side with a double-barreled H^+-sensitive microelectrode. At the first arrow the perfusate on the apical side was switched from control Ringer (CO_2-free and gassed in air) to a similar Ringer containing 15 mM NH_4Cl, and then, at the second arrow, it was subsequently returned to control 28 min later. NH_4Cl superfusion produced a rapid and long-lasting "plateau phase" intracellular alkalinization, which was followed 15 min later by a fall in pH_i. An abrupt "rebound" acidification occurred after NH_4Cl washout. The Na^+ transport rate and slope conductance increased with cellular alkalinization, whereas cell acidification produced a decrease in I_{sc} and g_a that closely followed the changes in pH_i. The inset shows the experimental set-up.

min of acid load (Figs. 5 and 6, and Table I), and thereafter increased for longer periods of intracellular acidosis. Conversely, an alkaline load increased P_{Na} and G_{Na} (Table I) and again the changes in $[Na]_i$ were biphasic and time dependent. Initially, during the intracellular alkalosis the $[Na]_i$ increased and after 5–10 min decreased. These biphasic effects of changing pH_i on the calculated $[Na^+]_i$ may be due to a pH

sensitivity of both apical Na^+ entry and basolateral Na^+ exit (via Na^+/K^+ ATPase). Another possibility is that pH_i-regulating mechanisms, such as Na^+/H^+ exchange, may modify the intracellular Na^+ transport pool (Ehrenfeld et al., 1987; Harvey and Ehrenfeld, 1988).

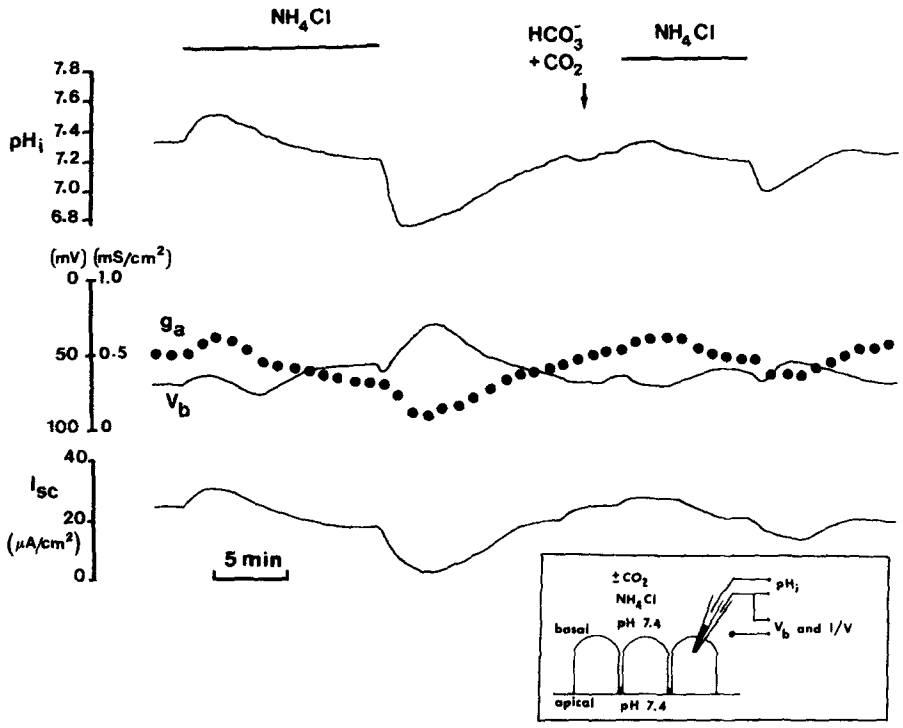

FIGURE 7. Response of pH_i, membrane potential, Na^+ conductance, and transport rate to the application of 15 mM NH_4Cl to the basolateral Ringer at a constant external pH 7.4 in the short-circuited isolated epithelium. Cell impalement was from the basolateral side with a double-barreled H^+-sensitive microelectrode. The addition of NH_4Cl to a CO_2-free Ringer gassed in air (first arrow) resulted in a transient intracellular alkalinization lasting 2–3 min, followed by a steady decrease in pH_i. A rapid rebound acidification occurred upon the removal of NH_4Cl. The changes in Na^+ conductance and transport rate were covariant with the variations in pH_i. Cell acidification produced a decrease, and alkalinization an increase, in these parameters. The effects of basolateral superfusion and washout of NH_4Cl on pH_i, g_a, and I_{sc} were considerably diminished when performed in a CO_2:HCO_3^--buffered Ringer on the basolateral side (record after HCO_3^-/CO_2 arrow). The inset shows the experimental protocol.

Dependence of g_b on pH_i

The *I-V* relations of the amiloride-sensitive current pathway across the basolateral cell membranes (I_b-V_b) were determined simultaneously with those of the apical cell membranes described above. The pattern of stimulation or inhibition of basolateral slope conductance after an intracellular alkali or acid load, respectively, was similar to that found for the apical cell membranes (Table I). The effect of a respiratory

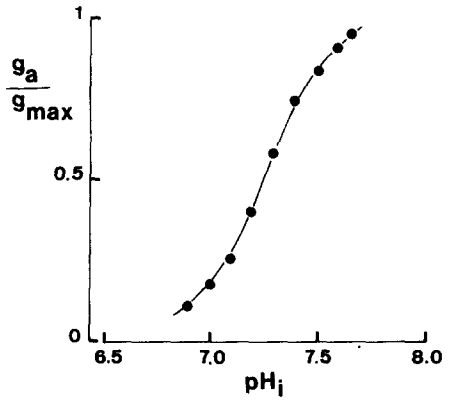

FIGURE 8. Apical membrane Na^+ conductance plotted as a function of pH_i (mean values in eight tissues). The g_a was determined from amiloride-sensitive *I-V* relations of the apical membrane as pH_i was varied at constant external pH by respiratory (CO_2) or metabolic (NH_4Cl) acid-base disturbances. Values of g_a were normalized by expressing them as a fraction of the maximum conductance measured at a pH_i of 7.75. The relation g_a/g_{max} vs. pH_i was best fit by a titration curve described by the equation:

$$g_a/g_{max} = (10^{-pK})^n/[(10^{-pK})^n + [H^+]_i^n] \quad (10)$$

giving a pK of 7.25, with $n = 2$, the number of protons interacting with each titratable site.

intracellular acid load on g_b was instantaneous. Evidence for the covariance of g_b with pH_i was obtained from simultaneous recordings of these parameters as a function of time (Fig. 9).

The response of g_b to changes in pH_i was just as rapid as that found for g_a, since the g_a and g_b described in Fig. 4, *A* and *B* were determined simultaneously and in the

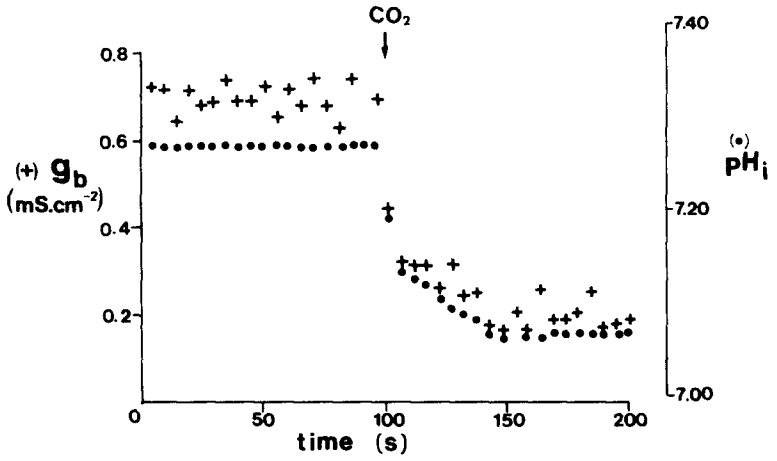

FIGURE 9. Computer print out of pH_i (●) and basolateral membrane conductance (+) (calculated every 5 s from circuit analysis), plotted as a function of time in the short-circuited frog skin. The record shows the rapid and covariant nature of pH_i and g_b variations after a respiratory acid load (at a constant external pH of 7.4) produced by switching from control Ringer (HCO_3^--free, gassed in air) to a Ringer buffered with CO_2:HCO_3 on the apical side. From this record an estimate of intrinsic (non–CO_2/HCO_3) intracellular buffering power (β_i) may be obtained from the change in pH_i of 0.21 units and the calculated $[HCO_3]_i$ of 9 mM (pCO_2 = 38 torr) to give a β_i of 45 slykes.

same cells. Therefore, both g_b and g_a vary in parallel with pH_i. The near constancy of *FR*a during acid-base disturbances supports this conclusion (Figs. 1–3).

The K^+ ion partial potential ratio (T_K) of the basolateral cell membranes showed a dependence on pH_i similiar to that found for g_b, and both parameters were extremely sensitive to pH_i, especially over the physiological range (Fig. 10). The best-fit curve relating g_b/g_{max} to pH_i gave a pK of 7.1 with two H^+ binding to each titration site. The I_b-V_b relations used to calculate g_b thus appear to provide a good description of the state of the K^+ conductive pathway and its pH_i dependence because of the close correlation between g_b and T_K.

DISCUSSION

Response of pH_i to Acid-Base Disturbances

We found that the effects of CO_2 and NH_4Cl (at constant external pH) on pH_i were dependent on the side of addition of the weak acid or base (Fig. 11). Apical applica-

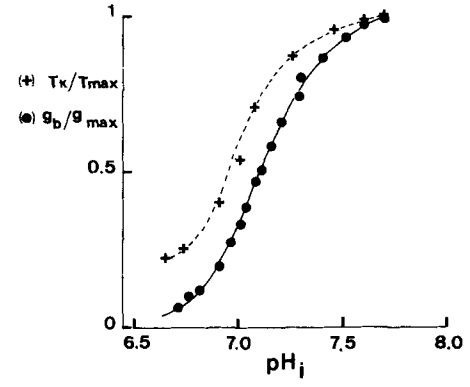

FIGURE 10. Normalized plots of basolateral membrane slope conductance (●) and K^+-dependent potential ratio (+) (equivalent in this case to K^+ transference), as a function of the pH; in eight isolated epithelia under short-circuit conditions. The g_b and T_K data were normalized by expressing them as a fraction of their maximum value determined at a pH_i of 7.75. The relation g_b/g_{max} (or T_K/T_{max}) vs. pH_i was best fit by the equation:

$$g_b/g_{max} \text{ (or } T_K/T_{max}) = (10^{-pK})^n/[(10^{-pK})^n + [H^+]_i^n] \quad (11)$$

with pK = 7.2 and n = 2 for g_b; and pK = 7.1 and n = 2 for T_K, respectively.

tion of CO_2/HCO_3^- Ringer caused an immediate and prolonged intracellular acidification, which was reversible upon the removal of CO_2/HCO_3. This response is similar to that found in the salamander proximal tubule (Boron and Boulpaep, 1983). The rapid acidification we observed could be explained by CO_2 entering the cells alone without HCO_3^- (Fig. 11 *A*). The increased pCO_2 within the cells would favor the formation of H^+ and HCO_3^-, and intracellular acidification would be maintained if HCO_3^- can subsequently leave the cells. We have previously shown that HCO_3^- efflux can occur across the basolateral cell membranes via a DIDS-sensitive Cl^-/HCO_3^- exchanger (Duranti et al., 1986). The asymmetry of the epithelium with respect to HCO_3^- permeability and the continuous loss of cell HCO_3^- via Cl^-/HCO_3^- exchange could provide an intracellular sink for CO_2, thus reinforcing the acid load.

For basolateral application of CO_2/HCO_3^- in the isolated epithelium, we usually observed an intracellular alkalinization after a rapid but small initial acidification. The HCO_3^- permeability of the basolateral membrane must be very high in order to

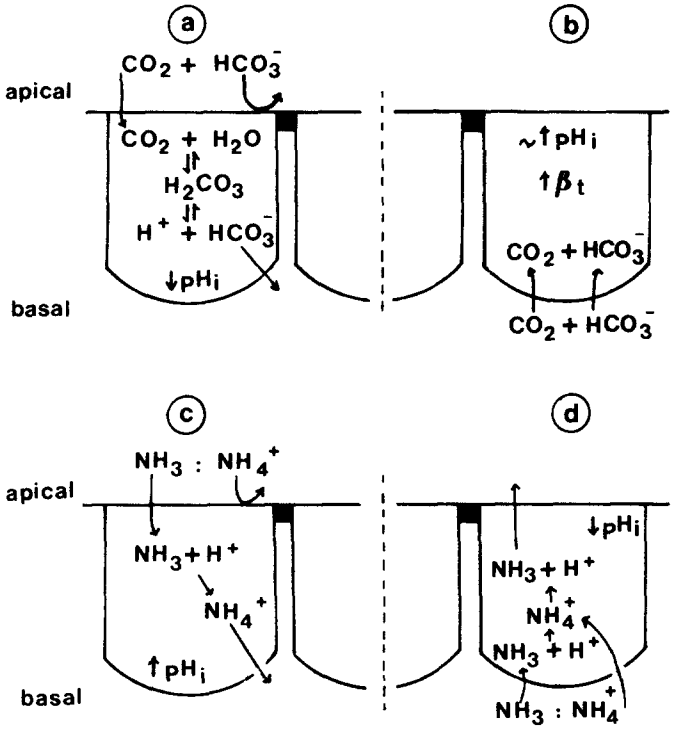

FIGURE 11. Schema of the experimental maneuvers designed to cause intracellular acid-base disturbances at constant external pH in frog skin epithelium. (*a*) The addition of CO_2:HCO_3-buffered Ringer solution to the apical side causes a rapid and prolonged intracellular acidification. The apical and basolateral membranes possess assymmetric permselectivity to HCO_3^-. Loss of HCO_3^- out across the basolateral membranes would tend to create an intracellular "sink" for CO_2 and thus reinforce the acid load. (*b*) CO_2:HCO_3 addition from the basolateral side increases pH_i slightly. Since both partners of the buffer pair enter the cell, the β_t is increased. (*c*) NH_4Cl addition from the apical side produces an immediate and prolonged intracellular alkalinization. The apical membrane is normally impermeable to K^+ and therefore NH_4^+ may not enter the cells from this side. The rapid diffusion of NH_3 into the cells will capture intracellular H^+, thus raising pH_i. Loss of NH_4^+ out across the basolateral membrane will favor the continued entry of NH_3 and cell alkalinization. (*d*) The addition of NH_4Cl from the basolateral side causes an initial transient intracellular alkalinization due to NH_3 entry. The basolateral cell membranes, however, are highly permeable to K^+ and NH_4^+ entry via K^+ channels is greatly favored by a large inward electrochemical driving force. Intracellular accumulation of NH_4^+ and its dissociation to NH_3 and H^+ will tend to acidify the cell and this process will be reinforced by NH_3 exit into the NH_4Cl-free apical solution.

counteract acidification arising from entry of CO_2 alone, and both partners of the buffer pair must have entered the cell almost simultaneously (Fig. 11 *B*). This would lead to an increase in the intracellular buffering power (see Appendix), which, of itself, may not change pH_i but could serve to limit cell acidification.

Apical application of NH_4Cl produced an intracellular alkalinization lasting up to 30 min, and rebound acidification occurred upon washout of the weak base. The pattern of these pH_i transients in response to NH_4Cl was similar to that described

for NH_4Cl exposure in mouse soleus muscle (Aickin and Thomas, 1977), giant barnacle muscle fibres (Boron, 1977), frog muscle (Bolton and Vaughan-Jones, 1977), squid giant axon (Boron and DeWeer, 1976), crayfish slow muscle fibers (Moody, 1980), crayfish neurons (Moody, 1981), and renal proximal tubule (Boron and Boulpaep, 1982). The prompt intracellular alkalinization in response to apical NH_4Cl exposure may be explained by the rapid entry of NH_3 and subsequent capture of cell H^+ (Boron and DeWeer, 1976). The NH_4^+ thus formed may leave the cell across the basolateral cell membranes (via K^+ channels) and thereby reinforce the intracellular alkalinization process (Fig. 11 *C*).

Exposure of the isolated epithelium to NH_4Cl from the basolateral side produced a biphasic pattern in the pH_i response similar to, but faster than that seen in apical application (Fig. 11 *D*). In this case, however, a rapid entry of NH_4^+ and accompanying intracellular acidification is to be expected since the basolateral membrane is highly permselective to K^+. Prolonged preexposure (>30 min) of the epithelium to NH_4Cl on the basolateral side produced a profound acidification. In this case, the recovery of pH_i, I_{sc}, and cell membrane conductances were delayed for periods of up to 1 h. Since a very high $[NH_4^+]_i$ is expected at equilibrium, an increase in cell volume may have complicated the response to long term NH_4Cl exposure. Finally, the magnitude of the pH_i changes induced by CO_2:HCO_3^- or NH_3:NH_4^+ also depends on the intracellular buffering power (see Appendix).

pH_i Effects on Cell Membrane Conductances

The amiloride-sensitive *I-V* curves of the apical cell membranes were accurately described by the GHK equation for Na^+ flux, in agreement with the findings reported for frog skin by DeLong and Civan (1984), Schoen and Erlij (1985), and other tight junction epithelia such as rabbit colon (Thompson et al., 1982), and *Necturus* and toad urinary bladder (Palmer et al., 1980; Thomas et al., 1983).

As was the case for the pH_i response, we found that the changes in the apical and basolateral membrane conductances depended on the side of the epithelium from which acid-base disturbances were induced. However, under short-circuit conditions, an intracellular acidification, no matter how produced, always caused an inhibition in Na^+ transport and in Na^+ and K^+ conductances. Likewise, an intracellular alkalinization always brought about an increase in these transport parameters.

Since I_{sc}, P_{Na}, g_a, g_b, and pH_i could be determined simultaneously, we were able to show that slight variations of pH_i in the physiological range (7.1–7.4) produced instantaneous and parallel changes in all these parameters. The relationship describing Na^+ and K^+ conductances as a function of pH_i could be fit by titration curves. Intracellular protons may titrate a charged group (at a pK of 7.2, histidine is a candidate) on the cytoplasmic side of the Na^+ and K^+ channels.

Previous studies have shown that Na^+ transport is sensitive to maneuvers designed to change pH_i. For example, CO_2 applied to the apical side at constant external pH was reported to inhibit Na^+ transport in frog skin (Funder et al., 1967; Mandel, 1978) and Na^+ conductance in K^+ depolarized toad urinary bladder (Palmer, 1985). However, Garty et al. (1985) recently reported that pH_i changes had no effect on amiloride-sensitive ^{22}Na fluxes in toad urinary bladder vesicles. This latter report is at variance with our findings in frog skin since unidirectional

^{22}Na influxes were inhibited by intracellular acidification (Table II). The reason for this discrepancy is not clear. Perhaps the sensitivity of the Na^+ channel is modified by the vesicle preparation procedure or perhaps hydrogen ions do not act directly on the channel but via a cytoplasmic mediator. The latter possibility seems unlikely because of the extreme rapidity of the pH_i effect in our study on whole epithelium and the recent report by Palmer and Frindt (1987) of the pH sensitivity of whole cell and cell-detached patch-clamped Na^+ channels in rabbit renal cortical collecting tubule.

Both the apparent K^+ conductance and basolateral membrane conductance were also found to be very sensitive to pH_i changes. This result agrees with previous reports on the effects of pH_i on K^+ conductances in excitable tissues, oocytes and epithelia. K^+ conductance was reported to be blocked by lowering pH_i in frog skeletal muscle (Blatz, 1980), starfish oocytes (Moody and Hagiwara, 1982), squid axon (Wanke et al., 1979), and in cultured bovine retinal pigment cells (Keller et al., 1986).

TABLE II

Effects of Intracellular Acid-Base Disturbances on Na^+ Influx in Frog Skin

Condition	$J_{13}^{^{22}Na}$ $neq \cdot h^{-1} \cdot cm^{-2}$	Difference from control
Control (30 min)	1,431 ± 173	—
NH_4Cl (20 min)	1,609 ± 185	+177* ± 43
NH_4Cl (50 min)	1,360 ± 142	−72(NS) ± 65
Washout (30 min)	839 ± 95	−593* ± 114

^{22}Na unidirectional influxes (apical to serosal) measured in frog skins ($n = 4$) during a control period lasting 30 min (control Ringer, pH 7.4 both sides), and in the presence of 15 mM NH_4Cl, to the apical Ringer at 20 and 50 min after addition, and 30 min after washout (return to control Ringer). The change in Na^+ fluxes are consistent with the variations in Na^+ conductance found in the experiment described in Fig. 6, as a result of NH_3/NH_4^+-induced plateau phase alkalinization and subsequent acidification, followed by rebound acidification after washout.

*Significantly different from control at level $P < 0.025$.

Our results indicate that, because of the high sensitivity of Na^+ and K^+ conductances to pH_i, pH_i is an important intrinsic regulator of transepithelial ion transport.

Transcellular Cross-Talk: pH_i as Mediator

Can intracellular H^+ act directly to effect changes in I_{sc}, and Na^+ and K^+ conductances or is there a secondary intracellular mediator involved? The possible role of cell Ca^{2+} as a regulator of epithelial Na^+ transport has recently been reviewed (Chase, 1984; Taylor and Windhager, 1985; Windhager et al., 1986; Frindt et al., 1988). Experimental maneuvers designed to increase $[Ca^{2+}]_i$ are reported to inhibit apical Na^+ entry (Grinstein and Erlij, 1978; Taylor and Windhager, 1979; Chase and Al-Awqati, 1983). It has been claimed that cell Ca^{2+} varies inversely with pH_i in nervous tissue (*Helix* neurons) (Meech and Thomas 1977, 1980), and such changes can influence membrane conductance (Meech, 1978). On the other hand, cell acidification has been reported to produce a fall in cell Ca^{2+} in *Helix* neurons (Alvarez-

Leefmans et al., 1981). Moreover, there are few data available on the relationship between pH_i and $[Ca^{++}]_i$ in epithelia, and the effect of changing pH_i on $[Ca^{++}]_i$ in excitable tissues are not consistent and cannot be predicted with certainty (for reviews see Moody, 1984; Busa, 1986). Palmer and Frindt (1987) recently reported that Ca^{2+} had no effect on the activity of patch-clamped cell-detached epithelial Na^+ channels. Moreover, we have found that the response of g_a and P_{Na} to an intracellular acid load in frog skin epithelium was similar in the presence of 20 mmol/liter Ca^{2+} or in a Ca^{2+}-free EGTA Ringer on the basolateral side, with or without the intracellular Ca^{2+} chelator MAPTAM ([bis-(2-amino-5-methyl-phenoxy)-ethane-*N,N,N',N'*-tetraacetic acid tetraacetoxymethyl ester]) and the Ca^{2+} ionophore ionomycin (Harvey and Thomas, 1987). This agrees with recent studies in which doubt was cast on the role of Ca^{2+} in controlling Na^+ transport in frog skin (Hogan et al., 1985; Nagel, 1987).

An increase in $[Na^+]_i$ has been proposed to act either directly or indirectly at the apical membrane to inhibit Na permeability (for review see Schultz, 1981). Here we found that changes in $[Na^+]_i$ (calculated from the I_a-V_a relations) during an acid load and the recovery phases were variable and tended to lag behind the changes in pH_i. We interpret the variations in $[Na^+]_i$ to result from pH_i-induced changes in Na^+ conductance and Na^+/K^+ ATPase activity. At the onset of an acid load the $[Na^+]_i$ decreased, possibly as a result of the decreased apical P_{Na}. As the acid load was prolonged, $[Na^+]_i$ increased; this may have been due to inhibition of the basolateral Na^+/K^+ ATPase. An increase in $[Na^+]_i$ at low pH_i could also occur from activated basolateral Na^+/H^+ exchange (Ehrenfeld et al., 1987; Harvey and Ehrenfeld, 1988). In these studies we showed that an acid load increases basolateral ^{22}Na uptake to 1,600 neq/$h^{-1}\cdot cm^{-2}$, which is in excellent agreement with the rate of Na^+ uptake calculated from changes in $[Na^+]_i$ (Figs. 4 and 5) at 5 mM/min corresponding to 1,800 neq/$h^{-1}\cdot cm^{-2}$ (for a volume to surface ratio of 6 $\mu l\cdot cm^{-2}$ (Harvey and Ehrenfeld, 1988). The gain in $[Na^+]_i$ despite reduction of g_a at acidic pH_i, is analogous to that found during ouabain inhibition of Na^+/K^+ ATPase in the presence of apical amiloride (Harvey and Kernan, 1984). These results support the conclusion that Na^+/K^+ ATPase is inhibited at acidic pH_i and that the gain in $[Na^+]_i$ occurs via stimulated basolateral Na^+/H^+ exchange. Increased $[H^+]_i$ is reported to reduce Na^+/K^+ ATPase activity (Eaton et al., 1984; Homareda and Matsui, 1985), which could lead to an increased $[Na^+]_i$ if apical Na^+ entry continued unrestricted. The sensitivity of P_{Na} to pH_i would serve to limit such a gain in $[Na]_i$. These effects are important in that previous studies have shown near constancy of $[Na^+]_i$ with increasing transport rate (Wills and Lewis, 1980; Thomas et al., 1983; Turnheim et al., 1983). For this to occur, the apical entry and basolateral extrusion of Na^+ must be kept in step. The signal for such transcellular coupling of ion movements may be pH_i.

APPENDIX

Intracellular Buffering Power

Weak acid method. Assuming that the initial change in pH_i upon superfusing the apical side with 5% CO_2 at constant external pH (24 mM HCO_3^-) is due solely to the entry of CO_2 and that HCO_3^- (OH^-) and H^+ do not cross the cell membranes during this time, then the

change in pH_i will depend on the intrinsic buffering power (β_i) of the cell and the initial pH_i. Thus the non-CO_2/HCO_3^- (intrinsic) buffering power may be calculated from $\beta_i = [HCO_3^-]_i/pH_i$. For the CO_2 application the calculated buffering power was 35 ± 4 meq H^+/pH unit ($n = 6$). Since CO_2 entry most likely gives rise to activation of pH_i regulatory mechanism(s) and basolateral HCO_3^- efflux, the calculation of β_i from the initial and final pH_i values may be erroneous. We therefore calculated β_i by taking the final pH_i value from the sharp peak obtained at the intersection of the tangent to the acidifying and plateau phases in response to a brief pulse of CO_2:HCO_3^--buffered Ringer.

Weak base method. In the absence of CO_2/HCO_3^- buffer, the buffering power calculated from the alkaline pH_i response to an NH_3/NH_4^+ load on the apical side also gives the intrinsic or non-NH_3/NH_4^+ buffering power. The magnitude of the NH_3-induced alkalinization is determined by the intrinsic buffering power $\beta_i = [NH^+]_i/pH_i$. The change in $[NH_4^+]_i$ was determined by taking the initial $[NH_4^+]_i$ to be zero and the final $[NH_4^+]_i$ to be $([NH_3] \cdot 10 \exp [pK - pH_i])$ with pK = 9.15. The value of β_i calculated by this method was 38 ± 4 meq H^+/pH unit ($n = 6$) and was not different from that determined by the weak acid method.

When a CO_2:HCO_3^- buffer is present and the cell membrane is permeable to both CO_2 and HCO_3^-, the total intracellular buffering power (β_t) is given by $\beta_t = \beta_i + \beta_{CO_2}$ where β_{CO_2} is the CO_2:HCO_3^- buffering power. For any pCO_2, β_{CO_2} is given by 2.3 ($[HCO_3]_i^2$). At a pH_i of 7.26 ± 0.03 and a 5% CO_2:24 mM HCO_3^- buffer on the basolateral side, the β_{CO_2} was 38 ± 5 meq H^+/pH unit ($n = 6$). This gives a β_t of 76 ± 9 meq H^+/pH unit ($n = 6$). Thus, in the presence of CO_2:HCO_3 Ringer solution on the basolateral side the β_t is doubled. Under these conditions we have seen that an acid load produced by basolateral $NH_3NH_4^+$ application produced small changes in pH_i (Fig. 7). For the case of apical applied CO_2 (which normally produces a large intracellular acidification), the pH_i response was practically abolished when the epithelium was previously bathed in CO_2:HCO_3^--buffered Ringer solution on the basolateral side (Figs. 1 and 5). The increase in β_t was produced only if CO:HCO_3^- Ringer was added to the basolateral side. Consequently, reduced effects of acid load on I_{sc} and conductances occur when compared with the effects produced when a CO_2:HCO_3^--free Ringer was present on the basolateral side. Under the latter conditions the addition of NH_4Cl to the apical side allows measurement of the total buffering power of the cell. Calculated in this way, $\beta_t = 80 \pm 7$ meq H^+/pH unit ($n = 4$), which agrees with the predicted value given above.

The authors wish to acknowledge the expert technical assistance of Corinne Raschi, Anny Giovagnoli, and Nicole Gabillat. Our thanks also to Pierre Guilbert for help in computer programming. The helpful criticism of Professor Roger Thomas of an an early draft of the manuscript is greatly appreciated.

This work was supported by research grants from the Centre National de la Recherche Scientifique (CNRS) (UA 638) and the Commissariat à l'Energie Atomique, France. B. J. Harvey and S. R. Thomas are career investigators of the CNRS France and J. Ehrenfeld is Maître de Conference at the University of Nice.

Original version received 26 May 1987 and accepted version received 22 April 1988.

REFERENCES

Aickin, C., and R. C. Thomas. 1977. Microelectrode measurement of the intracellular pH and buffering power of mouse soleus muscle fibres. *Journal of Physiology.* 267:791–810.

Alvarez-Leefmans, F. J., T. J. Rink, and R. Y. Tsien. 1981. Free calcium ions in neurones of *Helix aspersa* measured with ion-selective microelectrodes. *Journal of Physiology.* 315:531–548.

Blatz, A. L. 1980. Chemical modifiers and low internal pH block inward-rectifier K channels. *Federation Proceedings* 39:2073. (Abstr.)

Bolton, T. B., and R. J. Vaughan-Jones. 1977. Continuous direct measurement of intracellular chloride and pH in frog skeletal muscle. *Journal of Physiology.* 270:801–833.

Boron, W. F. 1977. Intracellular pH transients in giant barnacle muscle fibers. *American Journal of Physiology.* 233:C61–C73.

Boron, W. F., and E. Boulpaep. 1982. Hydrogen and bicarbonate transport by salamander proximal tubule cells. *In* Intracellular pH. Its Measurement, Regulation and Utilization in Cellular Functions. R. Nuccitelli and D. W. Deamer, editors. Alan R. Liss, New York. 253–267.

Boron, W. F., and E. Boulpaep. 1983. Intracellular pH regulation in salamander proximal tubules: Na-H exchange. *Journal of General Physiology* 81:29–52.

Boron, W. F., and P. De Weer. 1976. Intracellular pH transients in squid giant axons caused by CO_2, NH_3, and metabolic inhibitors. *Journal of General Physiology.* 67:91–112.

Busa, W. B. 1986. Mechanisms and consequences of pH-mediated cell regulation. *Annual Review of Physiology.* 48:389–402.

Chase, H. S. 1984. Does calcium couple the apical and basolateral membrane permeabilities in epithelia? *American Journal of Physiology.* 247:F869–F876.

Chase, H. S., Q. Al-Awqati. 1983. Calcium reduces the sodium permeability of luminal membrane vesicles from toad bladder. Studies using a fast reaction apparatus. *Journal of General Physiology.* 77:693-712.

Davis, C. W., and A. L. Finn. 1982. Sodium transport inhibition by amiloride reduces basolateral membrane K conductance in tight epithelia. *Science.* 216:525–527.

De Long, J., and M. M. Civan. 1984. Apical sodium entry in split frog skin current-voltage relationship. *Journal of Membrane Biology.* 82:25–40.

Diamond, J. M. 1982. Transcellular cross-talk between epithelial cell membranes. *Nature.* 300: 683–685.

Duranti, E., J. Ehrenfeld, and B. J. Harvey. 1986. Acid secretion through *Rana esculenta* skin: involvement of an anion-exchange mechanism at the basolateral membrane. *Journal of Physiology.* 378:195–211.

Eaton, D. C., K. L. Hamilton, and K. E. Johnson. 1984. Intracellular acidosis blocks the basolateral Na-K pump in rabbit urinary bladder. *American Journal of Physiology.* 247:F946–954.

Ehrenfeld, J., E. J. Cragoe, and B. J. Harvey. 1987. Evidence for a Na^+/H^+ exchanger at the basolateral membranes of the isolated frog skin epithelium: effect of amiloride analogues. *Pflügers Archiv.* 409:200–207.

Finn, A. L. 1974. Transepithelial potential difference in toad urinary bladder is not due to ionic diffusion. *Nature.* 250:495–496.

Frindt, G., C. O. Lee, J. M. Yang, and E. E. Windhager. 1988. Potential role of cytoplasmic calcium ions in the regulation of sodium transport in renal tubules. *Mineral Electrolyte Metabolism.* 14:40–47.

Funder, T., H. H. Ussing, and T. O. Wieth. 1967. The effects of CO_2 and hydrogen ions on active Na transport in the isolated frog skin. *Acta Physiologica Scandinavica.* 71:65–76.

Garty, H., E. D. Civan, and M. M. Civan. 1985. Effects of internal and external pH on amiloride blockable Na transport across toad urinary bladder vesicles. *Journal of Membrane Biology.* 87:67–75.

Grinstein, S., and D. Erlij. 1978. Intracellular calcium and the regulation of sodium transport in the frog skin. *Proceedings of the Royal Society of London.* 202:353–360.

Harvey, B. J., and J. Ehrenfeld. 1986. Regulation of intracellular sodium and pH by the electrogenic H^+ pump in frog skin. *Pflügers Archiv.* 406:362–366.

Harvey, B. J., and J. E. Ehrenfeld. 1988. Role of Na/H exchange in the control of intracellular pH and membrane conductances in frog skin epithelium. *Journal of General Physiology.* 92:793–810.

Harvey, B. J., and R. P. Kernan. 1984. Intracellular ionic activities in relation to external sodium and effects of amiloride and/or ouabain. *Journal of Physiology.* 349:501–517.

Harvey, B. J., and R. C. Thomas. 1987. Intracellular pH and calcium effects on sodium conductance and transport in isolated frog skin epithelium. *Journal of Physiology.* 353:C87. (Abstr.)

Helman, S. I., W. Nagel, and R. Fisher. 1979. Ouabain on active transepithelial Na transport by frog skin: studies with microelectrodes. *Journal of General Physiology.* 74:105–127.

Hogan, K., M. S. O'Mahony, and M. G. O'Reagan. 1985. Calcium and the regulation of sodium transport in frog skin. *Proceedings of the Royal Academy of Medicine (Ireland).* 154:325. (Abstr.)

Homareda, H., and H. Matsui. 1985. Effect of pH on Na^+ and K^+ binding to Na^+, K^+ ATPase. *In* The Sodium Pump. 4th International Conference on Na^+, K^+ ATPase. I. Glynn and C. Ellory, editors. The Company of Biologists. H. Charlesworth and Co., Huddersfield, England. 251–254.

Keller, S. K., T. J. Jentsch, M. Koch, and M. Wiederholt. 1986. Interactions of pH and K^+ conductance in cultured bovine retinal pigment epithelial cells. *American Journal of Physiology.* 250:C124–C137.

Kubota, T., B. A. Biagi, and G. Giebisch. 1983. Effects of acid-base disturbances on basolateral membrane potential and intracellular potassium activity in the proximal tubule of *Necturus*. *Journal of Membrane Biology.* 73:61–68.

MacRobbie, E. A. C., and H. H. Ussing. 1961. Osmotic behaviour of the epithelial cells of frog skin. *Acta Physiologica Scandinavica.* 53:348–365.

Mandel, L. J. 1978. Effects of pH, Ca, ADH and theophylline in kinetics of Na entry in frog skin. *American Journal of Physiology.* 235:C35–48.

Meech, R. W. 1978. Calcium dependent potassium activation in nervous tissues. *Annual Review of Biophysics and Bioengineering.* 7:1–18.

Meech, R. W., and R. C. Thomas. 1977. The effect of calcium injection on the intracellular sodium and pH of snail neurones. *Journal of Physiology.* 265:867–879.

Meech, R. W., and R. C. Thomas. 1980. Effect of measured calcium chloride injections on the membrane potential and internal pH of snail neurones. *Journal of Physiology.* 298:111–129.

Messner, G., W. Wang, M. Paulmichl, H. Oberleithner, and F. Lang. 1985. Ouabain decreases apparent potassium conductance in proximal tubules of the amphibian kidney. *Pflügers Archiv.* 405:131–137.

Moody, W. J. 1980. Appearance of calcium action potentials in crayfish slow muscle fibres under conditions of low intracellular pH. *Journal of Physiology.* 302:335–344.

Moody, W. J. 1981. The ionic mechanism of intracellular pH regulation in crayfish neurones. *Journal of Physiology.* 316:293–308.

Moody, W. J. 1984. Effects of intracellular H^+ on the electrical properties of excitable cells. *Annual Review of Neurosciences.* 7:257–278.

Moody, W. J., and S. Hagiwara. 1982. Block of inward rectification by intracellular H^+ in immature oocytes of the starfish *Mediaster aequalis*. *Journal of Physiology.* 79:115–130.

Nagel, W. 1987. On the origin of transport inhibition after omission of serosal sodium. *American Journal of Physiology.* 252:C623–C629.

Nagel, W., J. F. Garcia-Diaz, and A. Essig. 1983. Contribution of junctional conductance to the cellular voltage-divider ratio in frog skins. *Pflügers Archiv.* 399:336–341.

Palmer, L. G. 1985. Modulation of apical Na permeability of the toad urinary bladder by intracellular Na, Ca and H. *Journal of Membrane Biology.* 83:57–69.

Palmer, L. G., I. S. Edelman and B. Lindemann. 1980. Current-voltage analysis of apical sodium transport in toad urinary bladder. Effects of inhibitors of transport and metabolism. *Journal of Membrane Biology.* 57:59–71.

Palmer, L. G., and G. Frindt. 1987. Effects of cell Ca and pH on Na channels from rat cortical collecting tubule. *American Journal of Physiology.* 253:F333–F339.

Reuss, L., and A. L. Finn. 1975. Effects of changes in the composition of the mucosal solution on the electrical properties of the toad urinary bladder epithelium. *Journal of Membrane Biology.* 20:191–204.

Roos, A., and W. Boron. 1981. Intracellular pH. *Physiological Reviews.* 61:296–434.

Schoen, H. F., and D. Erlij. 1985. Current-voltage relations of the apical and basolateral membranes of the frog skin. *Journal of General Physiology.* 86:257–287.

Schultz, S. G. 1981. Homocellular regulatory mechanisms in sodium transporting epithelia avoidance of extinction by "flushthrough." *American Journal of Physiology.* 241:F579–F590.

Schultz, S. G., R. A. Frizzel, and H. N. Nellans. 1977. An equivalent electrical circuit model for sodium transporting epithelia in the steady state. *Journal of Theoretical Biology.* 65:215–229.

Taylor, A., and E. E. Windhager. 1979. Possible role of cytosolic calcium and Na-Ca exchange in regulation of transepithelial sodium transport. *American Journal of Physiology.* 236:F505–F512.

Taylor, A., and E. E. Windhager. 1985. Cytosolic calcium and its role in the regulation of transepithelial ion and water transport. *In* The Kidney, Physiology and Pharmacology. D. W. Seldin and G. Giebisch, editors. 1297–1322.

Thomas, R. C. 1984. Experimental displacement of intracellular pH and the mechanism of its subsequent recovery. *Journal of Physiology.* 354:3–22.

Thomas, S. R., Y. Suzuki, S. M. Thompson, and S. G. Schultz. 1983. Electrophysiology of *Necturus* urinary bladder. I. Instantaneous current-voltage relations in the presence of varying mucosal sodium concentrations. *Journal of Membrane Biology.* 73:157–175.

Thompson, S. M. 1986. Relations between chord and slope conductances and equivalent electromotive forces. *American Journal of Physiology.* 250:C333–C339.

Thompson, S. M., Y. Suzuki, and S. G. Schultz. 1982. The electrophysiology of rabbit descending colon. I. Instantaneous transepithelial current-voltage relations of the Na entry mechanism. *Journal of Membrane Biology.* 66:41–54.

Turnheim, K., S. M. Thompson, and S. G. Schultz. 1983. Relations between intracellular sodium and active sodium transport in rabbit colon: Current-voltage relations of the apical sodium entry mechanism in the presence of varying luminal sodium concentrations. *Journal of Membrane Biology.* 76:299–309.

Wanke, E., E. Carbone, and P. L. Testa. 1979. K^+ conductance modified by a titratable group accessible to protons from the intracellular side of the squid axon membrane. *Biophysical Journal.* 26:319–324.

Wills, N. K., and S. A. Lewis. 1980. Intracellular Na activity as a function of Na transport rate across a tight epithelium. *Biophysical Journal.* 30:181–186.

Windhager, E., G. Frindt, J. M. Yang, and W. Lee. 1986. Intracellular calcium ions as regulators of renal tubular sodium transport. *Klinische Wochenschrift.* 64:847–852.